# HPLC-MS and UV–Visible Coupled Analysis of Methylene Blue Photodegradation by Hydrothermally Grown ZnO Nanowires

Nathan Martin, Yamin Leprince-Wang

# HPLC-MS and UV-visible coupled analysis of methylene blue photodegradation by hydrothermally-grown ZnO nanowires

*N. Martin, Y. Leprince-Wang**

*ESYCOM Laboratory (UMR9007), Univ Gustave Eiffel, CNRS, 77454 Marne-la-Vallée Cedex 2 France*

**Corresponding author: yamin.leprince@univ-eiffel.fr*

## Abstract

Photocatalysis is an efficient and promising method to purify water. Numerous studies have been dedicated to demonstrate its efficiency on several hazardous compounds, derived from the food-processing, textile, and pharmaceutical industries. However, even if the degradation of such products has been extensively studied, obtaining information on their photodegradation pathway is still challenging, leading to concerns about the innocuousness of the treated water. In this study, we used ZnO nanowires (ZnO NWs), very efficient photocatalysts, thanks to their large surface/volume ratio, their chemical and thermic stability and their large band-gap ; to photodegrade a solution of the commonly used organic dye methylene blue (MB) under UV irradiation, followed simultaneously by UV-visible spectrometry and High-Performance Liquid Chromatography coupled with Mass Spectrometry (HPLC-MS). Coupling these two methods gave us real-time information on the photodegradation efficiency and degradation mechanism. The HPLC-MS analysis allowed us to confidently identify three reaction intermediates of the MB degradation: Azure A, B and C, as well as spot three other compounds, with uncertain formulas, leading to the presented hypothesis on the beginning of the MB degradation pathway. While the UV-visible analysis showed a total degradation of MB after 2h of photodegradation, the HPLC-MS analysis indicated that some MB remained in the solution. Its quantity was calculated to be 14 µg/L, which is harmless to humans, thanks to the external standard calibration method. Those results are therefore a proof of the excellent efficiency of our samples in water remediation, as well as a very interesting insight on the MB degradation mechanism.

**Keywords** HPLC-MS, UV-Visible, Methylene blue, Photocatalysis, ZnO nanowires, Degradation mechanism

## 1. Introduction

The steady growth of human population, estimated to reach almost 10 billion in 2050 [1], and climate change, put a huge pressure on Earth's natural resources, especially water. Thus, the management of today's water resources is crucial to ensure the availability of water of good quality in the future.

With the discovery of emerging pollutants, which effects on humans and environment are still unknown [2,3], new, efficient and ecological ways of depolluting water effluents are required.

Among all the solutions that can be used for water remediation, photocatalysis, with its theoretical ability to mineralize organic pollutants, using sunlight as its sole energy source, is one of the most promising [4,5]. This method requires the use of a photocatalyst, very often a metallic oxide such as ZnO or $TiO_2$ [6]. ZnO has the advantage of being produced from

abundant raw materials [7]. Furthermore, $TiO_2$ has been suspected of being carcinogenic by the American food and drug association [8,9], making ZnO a safer option to avoid risks to environment and/or to humans.

One of the easiest and widely used way of proving the efficiency of a photocatalyst on organic pollutants is degrading an organic dye and following the degradation efficiency by UV-visible (UV-vis) spectrometry [10,11]. This method is very useful to quickly know to which extend the degradation is efficient, but does not provide precise insight on the by-products or the remaining products in the reaction effluents, even if the final reaction mix is clear.

To increase the knowledge on the reaction mechanism and the composition of the reaction mix at the end of the photocatalysis, it is possible to use High-Performance Liquid Chromatography (HPLC), coupled with Mass Spectrometry (MS), to separate the components of the mix by chromatography and identify them according to the ratio between their mass and their electric charge, defined as the m/z ratio. This is a very efficient and powerful method [6], used for example to analyse the chemicals in medicinal herbs [12], produce new medicaments [13,14], or detect ones that have been counterfeit [15], but it requires much more preparation and equipment to be performed than UV-visible spectrometry.

Coupling both methods should then allow to obtain quick information on the advancement of the reaction, while having a good knowledge of the composition of the reaction mix, and identify the reaction intermediates produced during the reaction. As such, in this paper, we describe the photocatalytic degradation of Methylene Blue (MB), an organic dye often used to prove the photocatalytic efficiency of different compounds [7], using ZnO nanowires synthesized by a two-step hydrothermal method, and followed both by UV-vis and HPLC-MS.

## 2. Materials and Methods

The ZnO nanowires were synthetized by following an hydrothermal two-step method, as described in our previous works [16,17]. First, the substrate, a Si wafer, is cleaned by a surfactant solution in an ultrasonic bath, then dried in an oven for 20 minutes at 200°C. After 10 minutes in a plasma-cleaner (power high), the seed-layer, composed of a solution of Zinc acetate (Sigma-Aldrich, $Zn(Ac)_2$ dihydrate, > 98%) (1 g) in Polyvinylalcohol (Aldrich, 99%) (PVA) (10 g / 100 mL), is deposited onto the substrate by spin-coating, the substrate being then calcined at 500°C for 3h. In the second step, the substrate is placed in the growth solution (made of

equals volumes of a $Zn(NO_3)_2$ solution at 0.075 $mol \cdot L^{-1}$ and a HMTA solution at 0.0375 $mol \cdot L^{-1}$) for 4h at 90°C. Finally, the samples were annealed at 350°C for 30 minutes before being used. The obtained samples were studied under SEM observations, UV-vis absorption and X-Ray diffraction.

The photocatalysis were performed by degrading 30 mL of a solution of MB (Merck, Certistain Metyhlene Blue) at 10 $\mu mol \cdot L^{-1}$ under UV irradiation (Hamamatsu LC8, 365 nm). The samples were maintained at a distance of 10 cm from the lamp, and the solution was placed under agitation. The received UV irradiation power on the sample surface was estimated at 35 $mW.cm^{-2}$. Every fifteen minutes, the UV irradiation is stopped, and the absorbance of the solution is measured by an UV-vis spectrometer (Perkin-Elmer, Lambda 35), before being analysed by HPLC-MS. The remaining quantity of liquid is then poured again in the reaction mix, and the photocatalysis resumes. The whole process is repeated until the UV-visible measurements show that a plateau in the degradation rate is reached.

The HPLC-MS (Agilent 1260 Infinity II/6530 Mass Q-TOF LC/MS) is used in the following conditions: static phase: Zorbax C18 (reverse phase); mobile phase: acetonitrile 30%/aqueous ammonium acetate (0.05M) 70% (v/v); flowrate: 0.25 mL/min; injection volume: 200 µL; and polarity: negative.

## 3. Results and discussion

### 3.1 ZnO nanowires characterisation

**Figure 1(a)** shows the SEM images of our ZnO NWs samples. at 1100 ± 50 nm and their mean diameter at 85 ± 5 nm. As we can see, the NWs layer is largely homogenous, and the samples are similar to the ones obtained in our previous works, with a measured height of 1100 ± 50 nm and a measured mean diameter of 85 ± 5 nm [16,17].

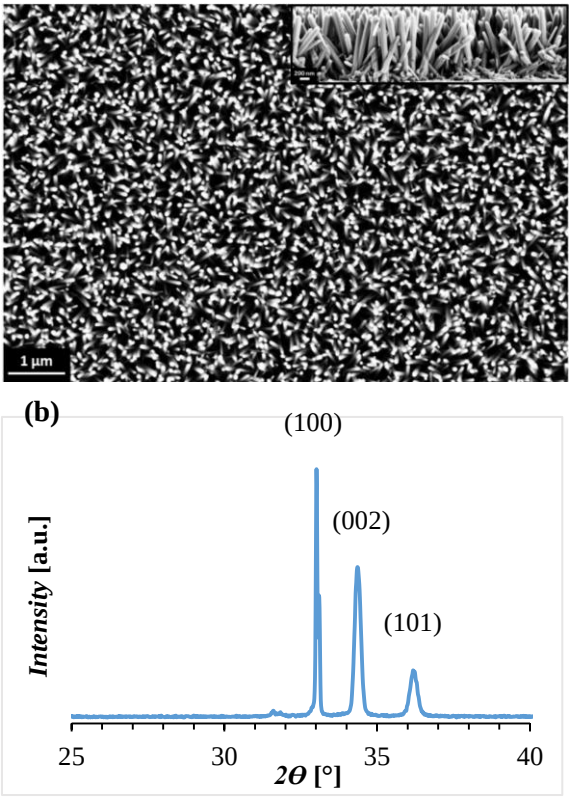


**Figure 1.** SEM image (a) and XRD pattern (b) of the as-obtained ZnO NWs.

**Figure 1(b)** displays the XRD pattern of the samples. The XRD peaks correspond to the usual ZnO pattern, meaning our samples exhibit a single-phase ZnO hexagonal Wurzite structure.

Finally, the UV-vis absorption results of our ZnO NWs were treated according to the Tauc-Lorentz model [18,19], and the obtained results yielded a band-gap value of 3.21 ± 0.1 eV.

### 3.2 Photodegradation results

The photodegradation results measured by UV-vis spectrometry from the beginning ($T_0$) to the end of the experiment ($T_{165}$) are presented in **Figure 2**. The degradation

(a) X, is calculated according to the following equation:

$$X_{(t)} = \frac{A_0 - A(t)}{A_0}.100\%$$

*Equation (1)*

where $A_0$ is the MB absorbance at the maximal absorption wavelength (664 nm) of the reaction mix before the start of the photodegradation and $A(t)$ is the MB absorbance at 664 nm at the time $t$ of the measurement. According to those results, the total degradation (X = 100%) is reached after 2h of photocatalysis (see **Figure 2(b)**).

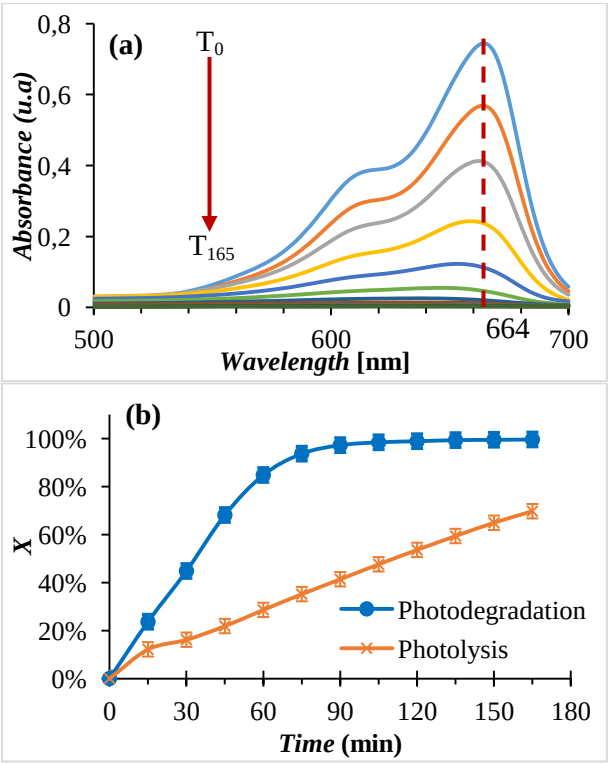


**Figure 2**. Evolution of the UV-vis spectra during the photodegradation (a) and corresponding evolution of the degradation

rate X (%) of MB compared to its photolysis (b).

### 3.3 HPLC-MS interpretation

The HPLC chromatogram and the MS spectra obtained at the beginning of the experiment is presented in **Figure 3**. The other chromatograms obtained during the experiment are available on the supplementary materials.

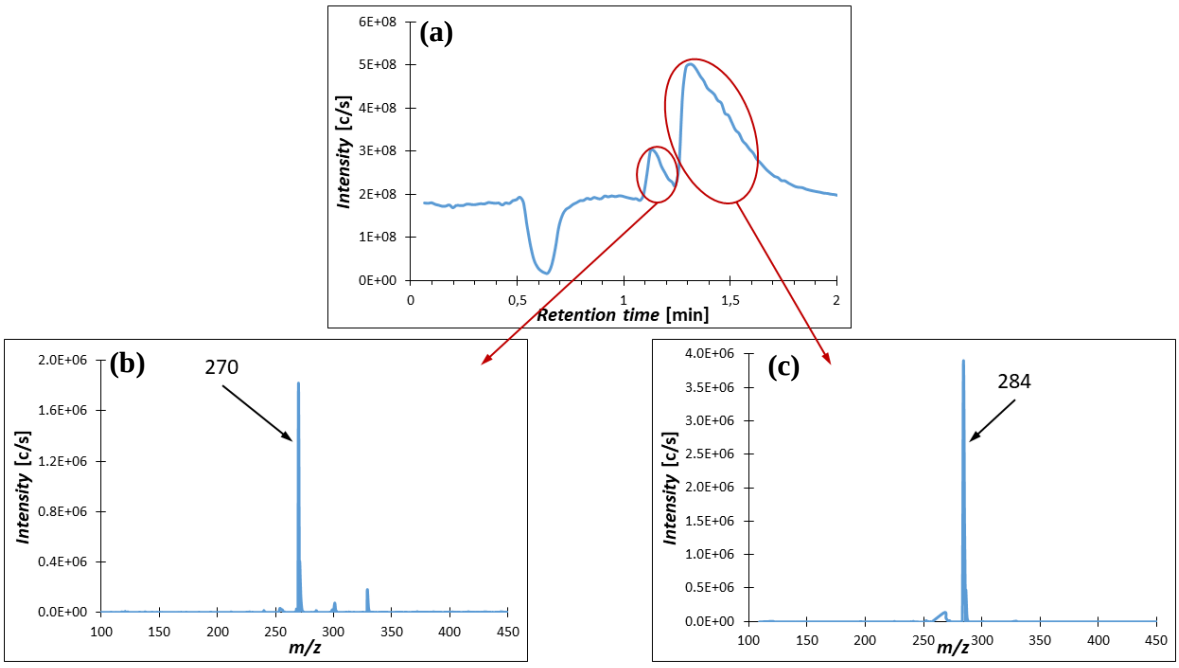


**Figure 3**. HPLC chromatogram (a) and corresponding MS spectra of the reaction mix at t=0, with first chromatogram peak spectrum (b), and second chromatogram peak spectrum (c).

Coupling HPLC and MS allows to identify the compounds corresponding to the chromatogram peaks, thanks to their m/z ratio. As can be seen in **Figure *3*(a)** the chromatogram at T = 0 displays two peaks. The first one (**Figure *3*(b)**) corresponds to a compound at 270 m/z, while the second one (**Figure *3*(c)**) corresponds to a compound at 284 m/z. According to the literature, the m/z ratio of MB is 284 m/z [20,21], and the m/z ratio of 270 can be attributed to Azure B, an oxidation product of MB [22,23], which formula is given in **Figure *4***. The red-marked H in **Figure *4*** highlights the difference between the two molecules. That way, we can follow the presence of Azure B and MB in the solution by monitoring the area of the first and second chromatogram peak, respectively.

The presence of Azure B before the beginning of the photocatalysis might be

due either to some impurities of the used reactant; or to the fact that, despite our best precautions, our MB solution has been exposed to light before the beginning of the experiment, leading to the production of Azure B in the solution by natural photodegradation.

As the photodegradation goes, we can note that the areas of the HPLC peaks corresponding to MB and Azure B decrease (**Table 1Erreur ! Source du renvoi introuvable.**). This confirms the result obtained with the UV-vis measurements that the MB is degraded during the photocatalysis. It also shows that Azure B is degraded along MB during the experiments.

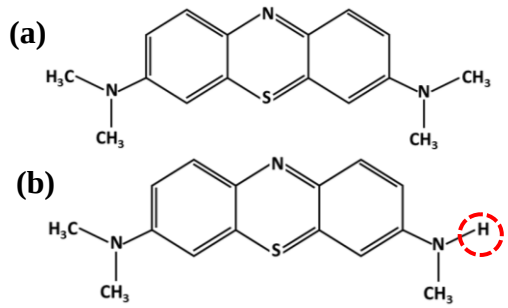


**Figure 4**. Formulas of MB (a) and Azure B (b).

During the photocatalysis, we see that two other peaks appear on the chromatogram (see supplementary materials **Figure S3** to **S6**): one can be attributed to a compound at 256 m/z, and one to a compound at 242 m/z. Those two compounds have been respectively identified as Azure A and Azure C, two by-products of the MB degradation already reported in literature [22,23]. Their corresponding chromatogram peaks intensity and area evolutions are resumed in **Table 1**. Their formulas can be seen in **Figure 5**. The two red-marked H in figure highlight the differences between the two molecules.

While they are detected in the HPLC-MS analysis, Azures A, B and C are not visible in the UV-Vis measurements. Our hypothesis is that it is due to two factors: the first one is that their wavelength of maximal absorption (650, 644 and 604 nm respectively for Azure A, B and C) is very close to the one of MB (664 nm). The second one is that their concentrations in the solution, as demonstrated by the area of the chromatogram peaks, stay lower than the one of MB (see **Table *1***). Thus, their absorption peaks on the UV-vis spectra are hidden in the MB absorption peak, explaining why they cannot be seen in the UV-vis spectra.

| Time [min] | m/z | Peak area (u.a) | Peak intensity (u.a x$10^6$) |
|---|---|---|---|
| 30 | 284 | $6.1x10^8$ | 38.0 |
| | 270 | $1.7x10^8$ | 26.0 |
| | 256 | $3.0x10^7$ | 3.80 |
| | 242 | $3.6x10^6$ | 0.70 |
| 45 | 284 | $4.9x10^8$ | 36.0 |
| | 270 | $1.8x10^8$ | 16.0 |
| | 256 | $4.2x10^7$ | 5.25 |
| | 242 | $4.5x10^6$ | 0.65 |
| 60 | 284 | $2.6x10^8$ | 26.0 |
| | 270 | $1.6x10^8$ | 16.0 |
| | 256 | $4.4x10^7$ | 5.30 |
| | 242 | $5.8x10^6$ | 0.90 |
| 75 | 284 | $1.1x10^8$ | 11.5 |
| | 270 | $9.5x10^7$ | 11.0 |
| | 256 | $3.8x10^7$ | 4.40 |

| | | | |
|---|---|---|---|
| (a) | 242 | $6.5x10^6$ | 0.70 |
| | 284 | $5.4x10^7$ | 5.50 |
| 90 | 270 | $4.5x10^7$ | 4.80 |
| | 256 | $2.1x10^7$ | 2.30 |
| | 242 | $4.9x10^6$ | 0.70 |
| | 284 | $2.0x10^7$ | 1.80 |
| 105 | 270 | $1.8x10^7$ | 1.60 |
| | 256 | $9.2x10^6$ | 0.90 |
| | 242 | $2.6x10^6$ | 0.35 |
| | 284 | $1.5x10^7$ | 1.30 |
| 120 | 270 | $1.0x10^7$ | 1.00 |
| | 256 | $5.1x10^6$ | 0.50 |
| | 242 | $1.4x10^6$ | 0.17 |
| | 284 | $5.2x10^6$ | 0.45 |
| 165 | 270 | $3.4x10^6$ | 0.29 |
| | 256 | $9.8x10^5$ | 0.10 |

**Table 1.** Evolution of the chromatogram peaks areas and intensity for the studied compounds during the photocatalytic process.

It is worth noting that some other compounds appear during the photodegradation (see supplementary materials, **Figures S4** to **S8** and **S10**). Among those compounds, the compound at 268 m/z can be attributed to MB having lost a methane [24,25]. According to literature [26-28], the compounds at 301 and 318 m/z might correspond to molecules with different formulas, as presented in **Figure 6Erreur ! Source du renvoi introuvable.**. Further researches are needed to find which of the different presented formulas are the ones actually produced during the experiments.

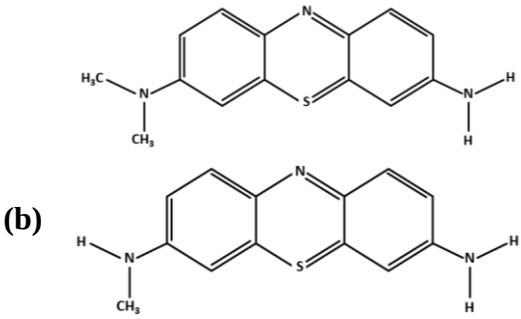

**Figure 5**. Formulas of Azure A (a) and Azure C (b).

Considering the other compounds have not been found in literature, and present a huge discrepancy in m/z values, we make the hypothesis that they are impurities of the solution, and not degradation intermediates or products. As for the molecules discussed above, further researches are needed to identify and classify them.

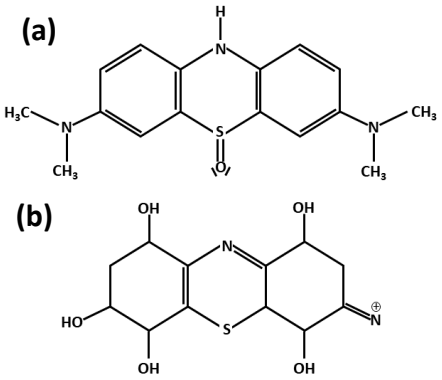

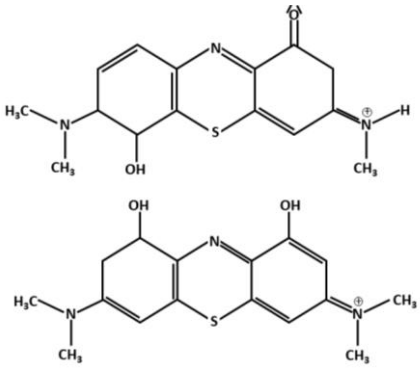


**Figure 6.** Presumed formulas of the molecules corresponding to 301 m/z: (a) Heitmann et al [26], (b) Gnaser et al [27] and at 318 m/z: (c) Castro et al [28], (d) Heitmann et al [26].

### 3.4 Degradation mechanism

As the areas of the chromatogram peaks are proportional to the concentration of the corresponding products, it is possible to estimate the evolution of the concentration of the different products during the experiments. To really calculate the concentration from the area of the chromatogram peaks, we need to previously calibrate the device to establish the calculation formula. As the only molecule we knew was going to be in the solution is MB, it is the only compound we performed a calibration for, using the external standard method. For the other compounds, only the concentrations of the Azures A, B and C could be estimated, as they are the only compounds which presented sufficiently high peak areas.

The evolution of the concentration of the degradation products (Azure A, B and C), is shown on **Figure 7**. It is worth noting that the concentration of every Azure first increases, then decreases during the course of the photodegradation. This seems to indicate that every studied product is produced during the reaction, then used, leading to the hypothesis that they are part of the photodegradation mechanism of the MB. We can also see that the different peaks reach their maximum intensity 15 min apart of each other, when the previously highest peak starts to decrease, which could be an indication that every Azure is produced from the previous ones, in the following order: Azure B, Azure A and Azure C.

For the other products, they might be part of the mechanism, or produced directly from the oxidation of MB, without taking part in the degradation mechanism.

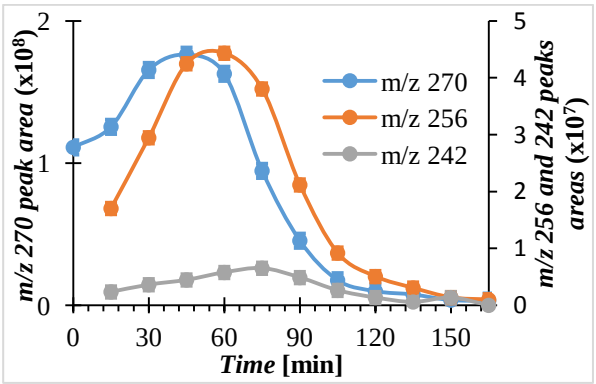


**Figure 7.** Evolution of the areas of the chromatogram peaks corresponding to the MS peaks at 270 m/z (Azure B), 256 m/z (Azure A) and 242 m/z (Azure C).

Those conclusions allow us to deduce what could be the beginning of the degradation mechanisms of MB in our conditions of photodegradation. Theses first steps are presented in **Figure 8**. Those steps are still hypothesis, and further experiments are needed to improve our comprehension of the degradation mechanism.

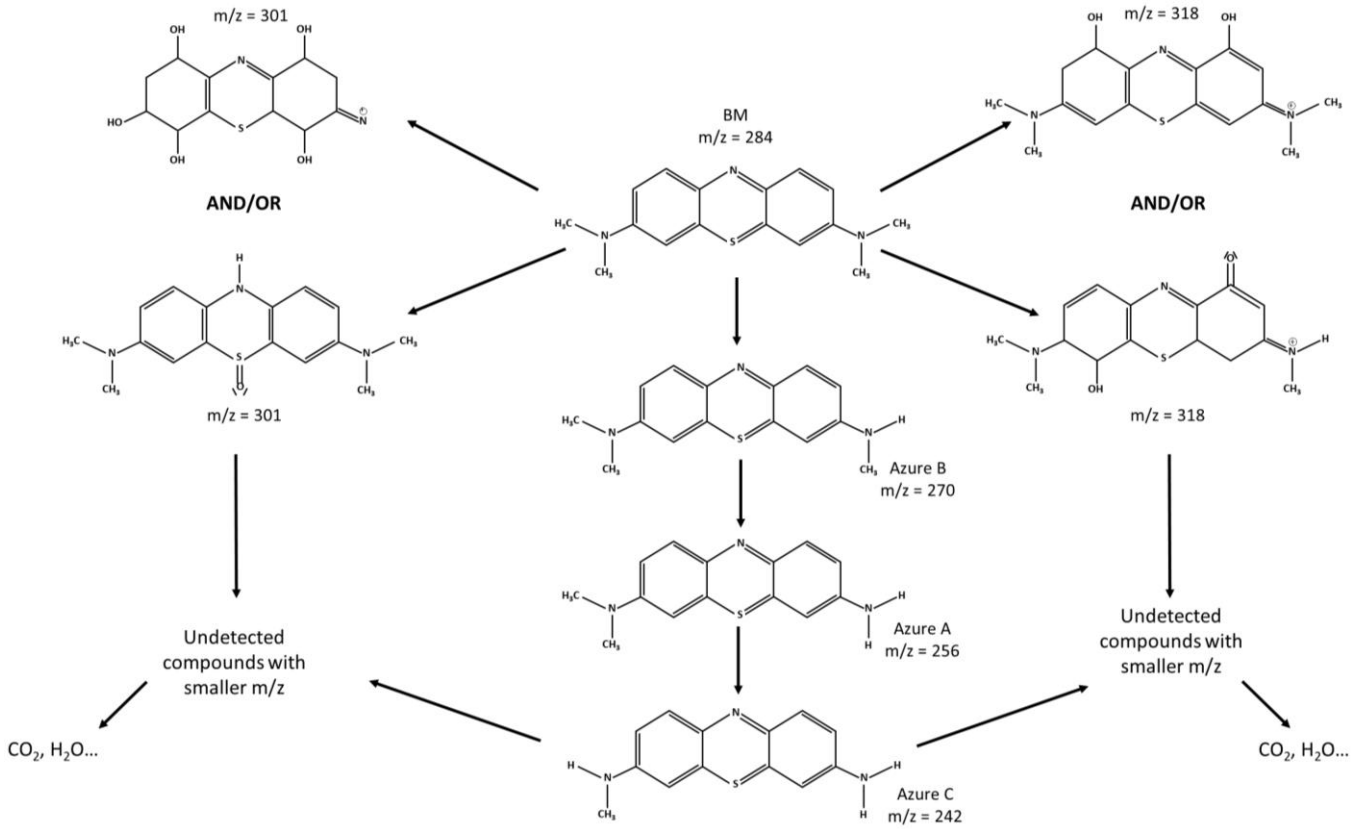


**Figure 8.** Beginning of the degradation mechanism of MB during the photodegradation.

### 3.5 Comparison between the analysis methods

The evolution of the calculated concentration of MB according to the two different analysis methods we used is indicated in **Figure 9**. If we compare the degradation rate curve we obtained by UV-Vis measurements and the one obtained by HPLC-MS analysis, we can see that the degradation rate is higher when measured by UV-Vis than by HPLC-MS. However, the two curves meet after 105 minutes of degradation, when the degradation rate reaches ~ 99%. As the HPLC-MS measurement should be the more precise of the two, it might be safe to assume that the UV-Vis measurement overestimates the degradation rate during the first part of the reaction. This might simply be due to the fact that the concentration of MB at the beginning of the photodegradation is supposed to be 10 $\mu mol \cdot L^{-1}$, whereas the

calculated concentration via HPLC-MS is inferior (6.8 µmol·L$^{-1}$), meaning that the calculated degradation rate will be less for the same concentrations during the experiment.

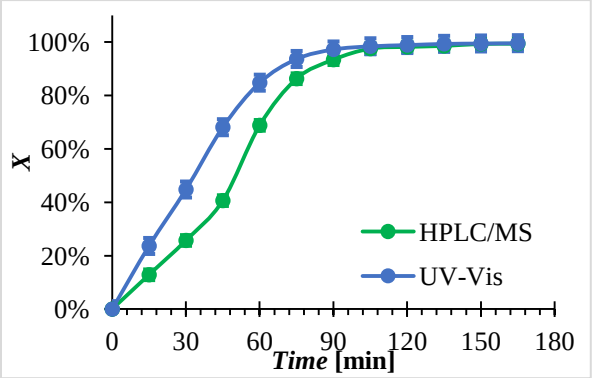


**Figure 9.** HPLC-MS and UV-visible photodegradation results of MB using ZnO nanowires as photocatalyst.

### 3.6 Estimation of the dangerousness of the solution effluents

The final concentration of MB was calculated to be around 0.043 µmol·L$^{-1}$, which corresponds to 14 µg·L$^{-1}$. The dangerous chronic exposure threshold of MB is of 5 mg·kg$^{-1}$ of corporal mass every day for 2 years for rats [29]. As the mean body mass of adults in the world is 62 kg [30], the treated water would thus be dangerous for adults if they drank 22 L of it every day for 2 years. As this value is vastly superior to the 1.5 L of water per day humans should drink, our effluents can be considered safe for adults. If we consider very young children, we can expect them to weight between 9 and 9.8 kg at age 1, meaning they should drink between 3.2 and 3.5 L of water every day for 2 years for the MB to be dangerous. Once again, this value is superior to the recommended quantity of water for children that age. Besides, the mass of children increases quickly at that age, further diminishing the risks. Thus, we can say that the remaining quantity of MB in the treated water is harmless, both to adults and to children.

## 4. Conclusion

We performed the photodegradation of MB using ZnO nanowires under UV irradiation. The UV-vis measurement showed that the MB was almost entirely degraded in about 2 hours, and the HPLC-MS analysis allowed us to gain insight on the beginning of the photodegradation process. Several degradation products have been detected. Three of them have been identified as Azure A, Azure B and Azure C. We also proposed several chemical formulas for three other products, but we were not able to firmly establish which molecules they were, or if they were degradation products or just impurities. Furthermore, the concentration of MB after the photodegradation was calculated as around 14 µg·L$^{-1}$, which, according to the chronic toxicity limits of MB, is safe.

Finally, we were able to compare the degradation results obtained from the UV-vis measurements and the ones calculated from the HPLC-MS results, and demonstrated that even when the UV-vis results show a total degradation, the HPLC-MS analysis is still able to detect MB in the reaction mix. This proves that HPLC-MS is a more accurate analysis, and that to obtain quantitative results, it is necessary to combine the two analyses.

Further investigations are needed to expand the knowledge on the detected molecules, especially the one that were not identified, as well as trying to detect the molecules that are produced from the degradation of Azure C in the reaction mix. The identification of the still unknown molecules can be performed by using an MS-MS method, whereas the detection of more molecules might be done by altering the HPLC-MS analysis conditions, especially, modifying the composition of the mobile phase, or imposing a concentration gradient during the injection of the sample.

## References


1. United Nations, Department of Economic and Social Affairs, Population Division, *World Population prospects 2019: Highlights*, **2019** *(ST/ESA/SER.A/423)*.
2. M. Raghav, S. Eden, K. Mitchell and B. White, *The Arroyo*, **2013**.
3. P. Verlicchi, M. Al Aukidy and E. Zambello, *Sci. Total Environ.*, **2012**, *429*, 123.
4. A. Laplanche, *Revue trimestrielle du réseau Ecrin*, **2005**, *60*, 20.
5. C. Byrne, G. Subramanian and S.C. Pillai, *J. Environ. Chem. Eng.*, **2018**, *6*, 3531.
6. C. Fernandez, M. Soledad Larrechi and M. Pilar Callao, *Trend. Anal. Chem.*, **2010**, *29(10)*, 1202.
7. K.M. Lee, C. W. Lai, K.S Ngai and J.C Juan, *Wat. Res.*, **2016**, *88*, 428.
8. S. Bettini, E. Boutet-Robinet, C. Cartier, C. Coméra, E. Gaultier, J. Dupuy, N. Naud, S. Taché, P. Grysan, S. Reguer, N. Thieriet, M. Réfrégiers, D. Thiaudière, J-P. Cravedi, M. Carrière, J-N Audiot, F.H. Pierre, L. Guyzlack-Piriou and E. Houdeau, *Sci. Rep.* **2017**, *7*, 40377.
9. IARC monographs on the evaluation of carcinogenic risks to humans, **2010**, *93*.
10. Y. G. Habba, M. Capochichi-Gnambodoe and Y. Leprince-Wang, *Appl. Sci.*, **2017**, *7*, 1185.
11. R. Saleh, N. F. Djaja, *Superlattice Microst.*, **2014**, *74*, 217.
12. D. Steinmann and M. Ganzera, *J. Pharm. Biomed. Anal.*, **2011**, *55*, 744.
13. B. L. Ackermann, M. J. Berna and A. T. Murphy, *Curr. Top. Med. Chem.*, **2002**, *2*, 53.

14. W. A. Korfmacher, *Drug Discovery Today*, **2005**, *20*, 1357.
15. R. Martino, M. Malet-Martino, V. Gilard and S. Balayssac, *Anal. Bioanal. Chem.*, **2010**, *398*, 77.
16. Y. G. Habba, M. Capochichi-Gnambodoe, L. Serairi and Y. Leprince-Wang, *Phys. Status Solidi B.*, **2016**, *253*, 1480.
17. C. Chevalier-César, M. Capochichi-Gnambodoe and Y. Leprince-Wang, *Appl. Phys. A*, **2014**, *115*, 953.
18. J. Tauc, R. Grigorovici and A. Vancu, *Phys. Status Solidi B.*, **1966**, *15*, 627.
19. T. Kamiya, K. Nomura and H. Hosono, *Phys. Status Solidi*, **2009**, *206*, 860.
20. G. J. Van Berkel, *Anal. Chem.*, **2002**, *74*, 6216.
21. V. K. Gupta, M. Sharma and R. K. Vyas, *J. Environ. Chem. Eng.*, **2015**, *3*, 2172.
22. S. Hisaindee, M. A. Meetani and M. A. Rauf, *Trends Anal. Chem.*, **2013**, *49*, 31.
23. T. B. Nguyen, R-A. Doong, C. P. Huang, C-W. Chen and C-D. Dong, *Sci. Total Environ.*, **2019**, *675*, 531.
24. D. J. Burinsky, R. L. Dilliplane, G. C. DiDonato and K. L. Busch, O*rg. Mass Spectrom.*, **1988**, *23*, 231.
25. J. M. Small and H. Hintelmann, *Anal. Bioanal. Chem.*, **2007**, *387*, 2881.
26. A. P. Heitmann, P. S. O. Patricio, I. R. Coura, E. F. Pedroso, P. P. Souza, H. S. Mansur and L. C. A. Oliveira, *Appl. Catal. B*, **2016**, *189*, 141.
27. H. Gnaser, M. R. Savina, W. F. Calaway, C. E. Tripa, I. V. Veryovkin and M. J. Pellin, *Int. J. Mass Spectrom.*, **2005**, *45*, 61.
28. C.S. Castro, M. C. Guerreiro, L. C. A. Oliveira, M. Gonçalves, A. S. Anastacio and M. Nazzarro, *Appl. Catal. A*, **2009**, *367*, 53.
29. S. S. Auerbach, D.W. Bristol, J. C. Peckham, G. S. Travlos, C. D. Hébert and S. Chhabra, *Food Chem. Toxicol.*, **2010**, *48*, 169.
30. S. C. Walpole, D. Prieto-Merino, P. Edwards, J. Cleland, G. Stevens and I. Roberts, *BMC Public Health*, **2012**, *12:439*.